

Local primary-and-multiple orthogonalization for leaked internal multiple crosstalk estimation and attenuation on full-wavefield migrated images

Zhang, Dong; Verschuur, D. J.; Davydenko, Mikhail; Chen, Yangkang; Alfaraj, Ali M.; Qu, Shan

DOI

[10.1190/geo2020-0448.1](https://doi.org/10.1190/geo2020-0448.1)

Publication date

2021

Document Version

Final published version

Published in

Geophysics

Citation (APA)

Zhang, D., Verschuur, D. J., Davydenko, M., Chen, Y., Alfaraj, A. M., & Qu, S. (2021). Local primary-and-multiple orthogonalization for leaked internal multiple crosstalk estimation and attenuation on full-wavefield migrated images. *Geophysics*, 86(1), A7-A13. <https://doi.org/10.1190/geo2020-0448.1>

Important note

To cite this publication, please use the final published version (if applicable).
Please check the document version above.

Copyright

Other than for strictly personal use, it is not permitted to download, forward or distribute the text or part of it, without the consent of the author(s) and/or copyright holder(s), unless the work is under an open content license such as Creative Commons.

Takedown policy

Please contact us and provide details if you believe this document breaches copyrights.
We will remove access to the work immediately and investigate your claim.

Local primary-and-multiple orthogonalization for leaked internal multiple crosstalk estimation and attenuation on full-wavefield migrated images

Dong Zhang¹, D. J. (Eric) Verschuur¹, Mikhail Davydenko¹, Yangkang Chen², Ali M. Alfaraj¹, and Shan Qu¹

ABSTRACT

An important imaging challenge is creating reliable seismic images without internal multiple crosstalk, especially in cases with strong overburden reflectivity. Several data-driven methods have been proposed to attenuate the internal multiple crosstalk, for which fully sampled data in the source and receiver side are usually required. To overcome this acquisition constraint, model-driven full-wavefield migration (FWM) can automatically include internal multiples and only needs dense sampling in either the source or receiver side. In addition, FWM can correct for transmission effects at the reflecting interfaces. Although FWM has been shown to work effectively in compensating for transmission effects and suppressing internal multiple crosstalk compared to conventional least-squares primary wavefield migration (PWM), it tends to generate relatively weaker internal multiples during modeling. Therefore, some

leaked internal multiple crosstalk can still be observed in the FWM image, which tends to blend in the background and can be misinterpreted as real geology. Thus, we adopted a novel framework using local primary-and-multiple orthogonalization (LPMO) on the FWM image as a postprocessing step for leaked internal multiple crosstalk estimation and attenuation. Due to their opposite correlation with the FWM image, a positive-only LPMO weight can be used to estimate the leaked internal multiple crosstalk, whereas a negative-only LPMO weight indicates the transmission effects that need to be retained. Application to North Sea field data validates the performance of the proposed framework for removing the weak but misleading leaked internal multiple crosstalk in the FWM image. Therefore, with this new framework, FWM can provide a reliable solution to the long-standing issue of imaging primaries and internal multiples automatically, with proper primary restoration.

INTRODUCTION

Internal multiples have drawn abundant interest for several decades due to the severe challenges in subsalt imaging and land data processing, where strong reflectors generate rich internal multiples to prevent interpreters from seeing the real geology. Many solutions have already been brought forward for internal multiple elimination in a data-driven manner. Inverse-scattering series-based approaches can predict all possible internal multiples that will be subtracted from the original data (Weglein et al., 1997). Layer-related internal multiple elimination is capable of estimating important subsets of interbed multiples by direct multidimensional convolution and cor-

relation of the surface data (Jakubowicz, 1998) or with the help of redatuming operators in which an approximated homogeneous velocity model is needed (Verschuur and Berkhout, 2005). Marchenko multiple elimination uses the Marchenko scheme to retrieve artifact-free primaries and accurately estimate all orders of internal multiples without any model knowledge and adaptive subtraction in theory (van der Neut and Wapenaar, 2016; Zhang and Slob, 2019). All of these data-driven methods require dense sampling in the sources and receivers, which is difficult to meet especially in a full 3D sense. Pica and Delmas (2008) introduce hybrid model- and data-based method for internal multiple prediction and attenuation. More recently, we have come to realize that full-wavefield

Manuscript received by the Editor 24 June 2020; revised manuscript received 27 August 2020; published ahead of production 4 October 2020; published online 16 December 2020.

¹Delft University of Technology, Department of Imaging Physics, Lorentzweg 1, 2628 CJ, Delft, The Netherlands. E-mail: d.zhang-3@tudelft.nl (corresponding author); d.j.verschuur@tudelft.nl; m.davydenko@tudelft.nl; a.m.a.alfaraj@tudelft.nl; s.qu@tudelft.nl.

²Zhejiang University, School of Earth Sciences, Zheda Road 38, 310027, Hangzhou, China. E-mail: yangkang.chen@zju.edu.cn.

© 2021 Society of Exploration Geophysicists. All rights reserved.

migration (FWM) including internal multiples in a model-driven manner might show promising potential to overcome the sampling issue in reality (Berkhout, 2014b; Davydenko and Verschuur, 2018). Specifically, FWM only needs dense sampling in either the source or receiver side, and the modeling strategy in FWM is redefined for imaging internal multiples. By allowing simulating transmission effects and multiple scattering in the subsurface through full-wavefield modeling (FWMMod) (Berkhout, 2014a), FWM reproduces the true physics and can better explain the internal multiples in the input data. Based on the estimated reflectivity model and given the migration velocity model, FWM handles all orders of internal multiples in a data-consistent and closed-loop fashion, without strong sampling requirements.

Davydenko and Verschuur (2018) demonstrate good performance of FWM on a North Sea field data set for attenuating internal multiple crosstalk that is overlying target reflections. Although FWM works effectively to compensate for transmission effects and suppress the internal multiple crosstalk compared with the conventional least-squares primary wavefield migration (PWM), it tends to underestimate the amplitudes of internal multiples during modeling. Therefore, some leaked internal multiple crosstalk is often observed in the FWM image, which might be interpreted as real geology and needs to be further attenuated. This can be regarded as a typical signal leakage problem. Zhang et al. (2020) propose local primary-and-multiple orthogonalization (LPMO) for successful surface-related multiple leakage extraction. Inspired by the aforementioned concept, we propose a novel framework using LPMO on the FWM image for leaked internal multiple crosstalk estimation and attenuation. PWM and FWM images are required to provide the difference image that consists of coupled transmission effects and initially estimated internal multiples. Application to the same Vøring field data as shown by Davydenko and Verschuur (2018) validates the promising performance of the proposed framework.

FWM AND ITS MODELING ENGINE FWMMod

To better understand the physics behind FWM and its advantages, a brief introduction of FWM and its modeling engine FWMMod is given in this section. The objective function for FWM can be written as follows:

$$J_{\text{FWM}} = \frac{1}{2} \sum_{\omega} \sum_{\text{shots}} \|\mathbf{d}_{\text{obs}}^-(z_0) - \mathbf{p}^-(z_0, \hat{\mathbf{r}})\|_2^2, \quad (1)$$

where $\mathbf{d}_{\text{obs}}^-(z_0)$ and $\mathbf{p}^-(z_0, \hat{\mathbf{r}})$ represent the monochromatic observed and modeled upgoing wavefield at the surface z_0 for a single shot, respectively, and $\hat{\mathbf{r}}$ denotes the reflectivity parameter as a function of subsurface coordinate that needs to be estimated during FWM. Equation 1 can be augmented by an extra constraint term, for example, a sparsity constraint. In terms of objective functions, FWM is similar to most least-squares-type migrations and can be solved by gradient-based approaches (Davydenko and Verschuur, 2018). However, the unique feature and power of FWM lie in its modeling engine FWMMod, which takes multiple scattering and transmission effects into account, based on the estimated image. First, FWMMod describes the two-way wavefield via one-way wavefields, that is, the downgoing and upgoing wavefields. Migration velocity and reflectivity are decoupled to diminish nonlinearity. Multiple-scattered

reflections and transmission effects are handled at each depth level z_n in an elegant way (Berkhout, 2014a):

$$\begin{aligned} \mathbf{q}^+(z_n) &= \mathbf{s}^+(z_n) + \mathbf{T}^+(z_n)\mathbf{p}^+(z_n) + \mathbf{R}^\cap(z_n)\mathbf{p}^-(z_n), \\ \mathbf{q}^-(z_n) &= \mathbf{s}^-(z_n) + \mathbf{T}^-(z_n)\mathbf{p}^-(z_n) + \mathbf{R}^\cup(z_n)\mathbf{p}^+(z_n), \end{aligned} \quad (2)$$

where $\mathbf{p}^\pm(z_n)$, $\mathbf{q}^\pm(z_n)$, and $\mathbf{s}^\pm(z_n)$ denote the incoming, outgoing, and source wavefields; superscripts + and - refer to downgoing and upgoing, respectively; $\mathbf{T}^\pm(z_n)$ represents the transmission matrix; and $\mathbf{R}^\cup(z_n)$ and $\mathbf{R}^\cap(z_n)$ represent the upward and downward reflection matrix, respectively. Moreover, the wavefield propagation between two adjacent depth levels z_n and z_{n-1} is described by propagation matrices $\mathbf{W}(z_n, z_{n-1})$ and $\mathbf{W}(z_{n-1}, z_n)$:

$$\begin{aligned} \mathbf{p}^+(z_n) &= \mathbf{W}(z_n, z_{n-1})\mathbf{q}^+(z_{n-1}), \\ \mathbf{p}^-(z_{n-1}) &= \mathbf{W}(z_{n-1}, z_n)\mathbf{q}^-(z_n). \end{aligned} \quad (3)$$

Equations 2 and 3 introduce the basic ingredients of FWMMod. We recursively repeat this process from the surface to the bottom and vice versa, referred to as one round trip. Only primary reflections are generated during the first round trip. Multiple scattering will be successfully modeled as the number of round trips increases. In this way, surface-related multiples, internal multiples, and transmission effects can be taken into account during modeling, and, via inversion, the recovered reflectivity is optimized (Berkhout, 2014b).

LPMO FOR LEAKED INTERNAL MULTIPLE CROSSTALK ESTIMATION AND ATTENUATION

LPMO has shown promising results in surface-related multiple leakage estimation (Zhang et al., 2020). In this paper, we propose leaked internal multiple crosstalk estimation and attenuation using LPMO. Two clear differences from the surface-related multiple case are (1) instead of a data-domain (e.g., shot or offset domain) estimation for surface multiple leakages, the leaked internal multiple crosstalk is estimated in the image domain, that is, the FWM image and (2) initially estimated internal multiples are coupled with transmission effects, unlike estimated surface multiples. The main advantage for image-domain LPMO is that the noise is already canceled by the summing process in FWM and a better grip on the internal multiples can be obtained (Wang et al., 2011). However, FWM also changes all of the primary contributions due to the restored transmission effects; therefore, to minimize the coupled transmission effects on leaked internal multiple crosstalk estimation is the new challenge. Based on the PWM and FWM images, we rearrange the basic relations in vector notation:

$$\begin{aligned} \mathbf{r}_{\text{PWM}} &= \mathbf{r}_{\text{FWM}} + \mathbf{r}_{\text{diff}}, \\ \mathbf{r}_{\text{diff}} &= \mathbf{r}_{\text{TE}} + \mathbf{r}_{\text{IM}}, \end{aligned} \quad (4)$$

where \mathbf{r}_{PWM} and \mathbf{r}_{FWM} denote the vectorized PWM and FWM images, respectively. The differences \mathbf{r}_{diff} between two images consist of two parts: the transmission effects \mathbf{r}_{TE} and the initially estimated internal multiples \mathbf{r}_{IM} by FWM. Due to its tendency to estimate relatively weaker internal multiples, the FWM image still contains some visible leaked internal multiple crosstalk. Our goal is to use the initially estimated internal multiples \mathbf{r}_{IM} to match and extract the leaked internal multiple crosstalk in the FWM image. However, the initially estimated internal multiples cannot be easily separated

from the difference image. Therefore, we match the leaked internal multiple crosstalk with the differences between FWM and PWM in a least-squares sense:

$$\min_{\mathbf{w}} \|\mathbf{r}_{\text{FWM}} - \mathbf{w} \circ \mathbf{r}_{\text{diff}}\|_2^2, \quad (5)$$

where \mathbf{w} denotes the LPMO weight and \circ represents the Hadamard product (element-by-element multiplication). With the help of a smoothness constraint, the above unconstrained minimization problem can be solved by a shaping regularization-based inversion scheme (Fomel, 2007b):

$$\mathbf{w}^+ = \mathcal{FH}([\lambda^2 \mathbf{I} + \mathcal{T}(\mathcal{D}^T \mathcal{D} - \lambda^2 \mathbf{I})]^{-1} \mathcal{T} \mathcal{D}^T \mathbf{r}_{\text{FWM}}), \quad (6)$$

where $\mathcal{D} = \text{diag}(\mathbf{r}_{\text{diff}})$, λ is a scaling parameter, and $[\cdot]^T$ denotes the matrix transpose. Here, \mathcal{T} , \mathcal{H} , and \mathcal{F} represent the triangular smoothing, thresholding, and median filtering operators, respectively. Note that due to the nonseparability between the initially estimated internal multiples and transmission effects, the whole inversion framework not only matches the leaked internal multiple crosstalk with initially estimated internal multiples \mathbf{r}_{IM} , but also the primaries in the FWM image with transmission effects \mathbf{r}_{TE} . However, FWM tends to estimate stronger events to compensate for the transmission effects, and it typically underestimates the internal multiples, which leads to an opposite correlation in the difference image compared to the FWM image, that is, a positive correlation for the leaked internal multiple crosstalk and a negative correlation for the transmission effects. Therefore, we could take advantage of this prior knowledge by using a positive-only LPMO weight through a thresholding operator. In this way, \mathbf{w}^+ indicates the estimated positive-only LPMO weight that is related to the leaked internal multiple crosstalk \mathbf{r}_{LIM} in the FWM image:

$$\mathbf{r}_{\text{LIM}} = \mathbf{w}^+ \circ \mathbf{r}_{\text{diff}}. \quad (7)$$

Thus, we obtain relations for the final estimated FWM and difference images:

$$\begin{aligned} \hat{\mathbf{r}}_{\text{FWM}} &= \mathbf{r}_{\text{FWM}} - \mathbf{w}^+ \circ \mathbf{r}_{\text{diff}} = \mathbf{r}_{\text{FWM}} - \mathbf{r}_{\text{LIM}}, \\ \hat{\mathbf{r}}_{\text{diff}} &= \mathbf{r}_{\text{diff}} + \mathbf{w}^+ \circ \mathbf{r}_{\text{diff}} = \mathbf{r}_{\text{TE}} + \hat{\mathbf{r}}_{\text{IM}}, \end{aligned} \quad (8)$$

where $\hat{\mathbf{r}}_{\text{FWM}}$, $\hat{\mathbf{r}}_{\text{diff}}$, and $\hat{\mathbf{r}}_{\text{IM}}$ are the final estimated FWM image, difference image, and internal multiples after LPMO, respectively.

RESULTS

The Vøring field data set from the Norwegian North Sea is used to test the proposed framework. Davydenko and Verschuur (2018) demonstrate the ability of FWM for handling internal multiples on the same data set, and detailed preprocessing steps and data information can be found therein. Note that these data are particularly suited for internal-multiple-related research due to a large water depth and, therefore, the absence of surface-related multiples in the target area.

We start with the PWM, FWM, and their difference images as shown in Figure 1a, 1b, and 1c, respectively. Generally, it is clear that there are mostly flat layers above 2.2 km in depth and dipping layers below this level. Due to the conflicting dips below the anticline in Figure 1a ranging from 2.3 to 2.7 km, the crosstalk from internal multiples is obvious in the PWM image, as indicated by the

arrows. Because of the modeling advantages for taking the internal multiples and transmission effects into consideration, FWM shows significant internal multiple crosstalk attenuation, as indicated by the arrows from the same area in Figure 1b. Even some crosstalk events above 2 km, indicated by the arrows, are slightly suppressed. However, the leaked internal multiple crosstalk in Figure 1b still hinders geologic interpretation. Figure 1c clearly demonstrates the differences between the PWM and FWM images, where the initially estimated internal multiples and transmission effects are visible. Due to their opposite correlation in the difference image compared to the FWM image, the LPMO weight related to leaked internal multiple crosstalk can be obtained by considering a positive-only weight (Figure 1d). The locations of the leaked internal multiple crosstalk can be well detected in the estimated LPMO weight. Figure 1e displays the final estimated FWM image after LPMO, where the leaked internal multiple crosstalk is further attenuated, especially for the areas indicated by the arrows. The same image improves significantly when compared directly to the PWM image. Figure 1f demonstrates the difference image after LPMO that extracts the leaked internal multiple crosstalk as shown by the arrows, whereas transmission effects are untouched. Note that because of the tendency of FWM to underestimate internal multiples, the LPMO weight for leaked internal multiple crosstalk estimation tends to be larger than the surface-related multiple case (Zhang et al., 2020). For these data, the LPMO weight ranges from 0 to 5. Special attention should be paid on the median filtering operator inside LPMO because there exists a trade-off for the window size of the median filter. The edge effect starts to become severe with smaller window sizes, whereas the multiple attenuation performance degrades with larger window sizes. We use 5×3 samples as our window size for these field data.

To better understand the power of FWM on compensating for transmission effects and attenuating internal multiple crosstalk and also to better demonstrate the LPMO performance on the FWM image, a zoom-in trace comparison is given in Figure 2a. It is obvious that the FWM trace (the red line) has a stronger amplitude than the PWM trace (the black line) especially above 2.2 km, which indicates that transmission effects are taken into account by FWM. As for the target area ranging from 2.2 to 2.5 km, the FWM trace significantly attenuates the internal multiple crosstalk compared to the PWM trace. However, the leaked internal multiple crosstalk is still visible from the FWM trace, which means that the FWM-estimated internal multiples are weaker than the real ones. The FWM trace after LPMO (the green line) from the zoom-in trace comparison shows further attenuation for the leaked internal multiple crosstalk, while retaining all of the transmission effects, which indicates the effectiveness of the proposed framework. We also provide the FWM and the difference image similarity map (Fomel, 2007a; Chen and Fomel, 2015) comparison before and after using LPMO on the FWM image in Figure 2b and 2c for a clearer demonstration. It is also obvious from the similarity maps that the leaked internal multiple crosstalk on the FWM image has been effectively attenuated, as indicated by the arrows.

To QC the retained transmission effects, we display the negative-only LPMO weights in Figure 2d. The negative LPMO weights (the blue area) are in good agreement with most layer structures, where most of the transmission effects are generated. Thus, layer-structured primaries can be well-preserved by simply rejecting the negative LPMO weight.

However, using conventional L_2 -norm adaptive subtraction to match the leaked internal multiple crosstalk with the difference image will cause severe primary damage due to not accounting for transmission effects. This is shown in Figure 2e, where the primary damage occurs across the whole image. Moreover, some leaked internal multiple crosstalk is still visible after L_2 -norm adaptive subtraction of the difference image in Figure 1c. In addition, the transmission effects in Figure 2f mistakenly extract the primary energy during L_2 -norm adaptive subtraction. This is because the

L_2 -norm-based matching filter can be easily updated to match the negatively correlated transmission effects, which usually happen to primaries.

To test the robustness of the proposed framework using LPMO on the FWM image, an extra experiment is applied on the same field data set, but with 3% velocity errors. From the PWM, FWM and their difference images in Figure 3a, 3b, and 3c, the internal multiple crosstalk indicated by the arrows can still be attenuated to some extent although the whole image is slightly shifted due

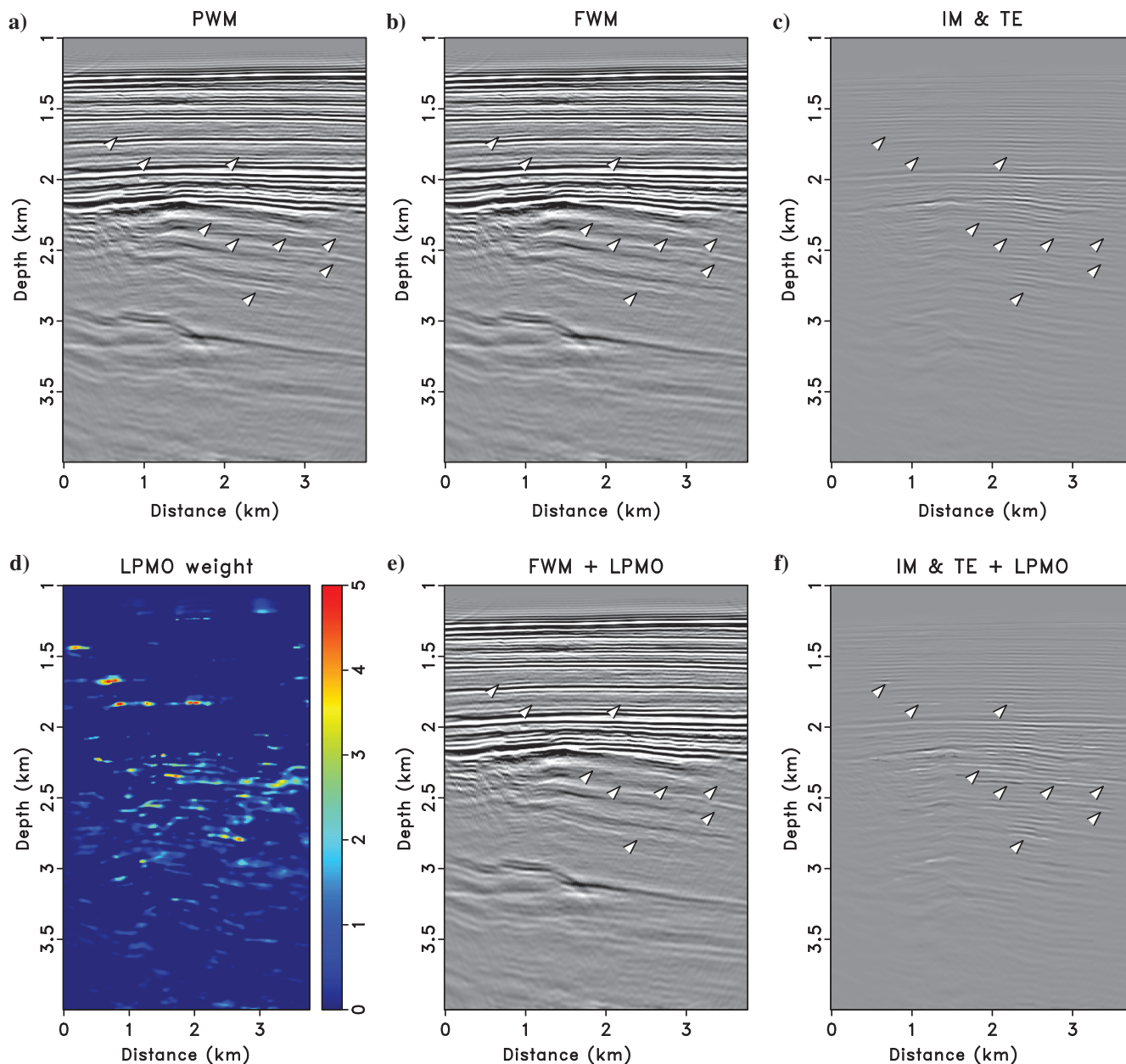


Figure 1. LPMO on the FWM image of the Vøring field data set: (a) PWM image, (b) FWM image, (c) the difference image between PWM and FWM that includes the initially estimated internal multiples (IM) and transmission effects (TE), (d) estimated positive-only LPMO weight related to the leaked internal multiple crosstalk in the FWM image, (e) final estimated FWM image after LPMO, and (f) the difference image that includes the final estimated internal multiples and transmission effects after LPMO.

to the velocity errors. Transmission effects and internal multiples can again be observed from the difference image. By accepting positive-only LPMO weight, the leaked internal multiple crosstalk can be detected in Figure 3d. Figure 3e and 3f shows the FWM and difference images after LPMO, respectively. We can observe that the leaked internal multiple crosstalk from the final estimated FWM image is further attenuated, whereas the estimated internal multiples extract their leaked energy in the final estimated difference image.

DISCUSSION

The FWM methodology is a very promising method that aims at solving a long-standing issue in imaging technology: including the internal multiples as part of the imaging scheme. In this way, the traditional multiple removal and the subsequent primary imaging method are being replaced by one inversion-type imaging process that handles all internal multiples on the fly. However, this technology sometimes struggles to find the exact balance between

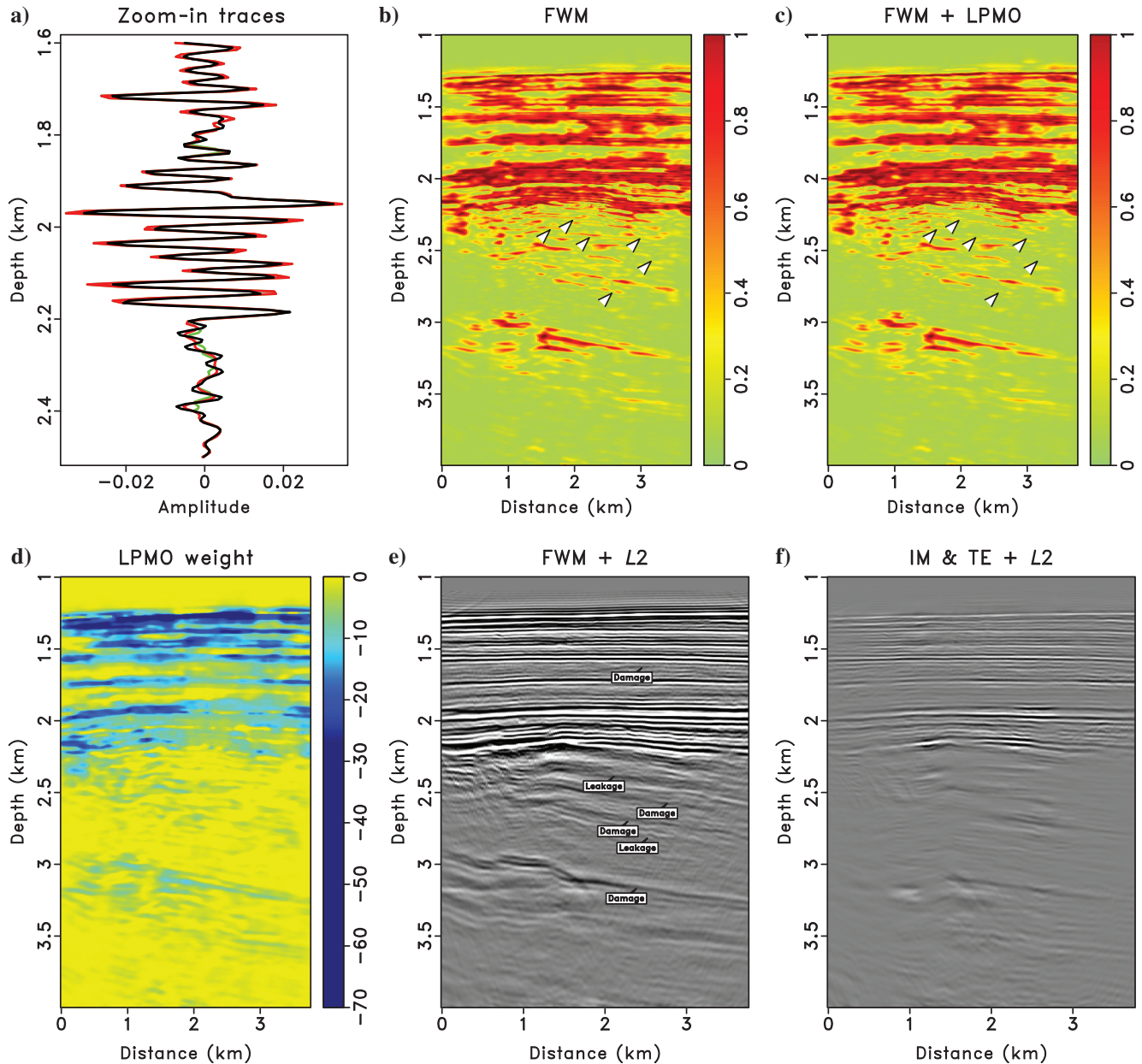


Figure 2. (a) A magnified trace comparison at 2.2 km ranging from 1.6 to 2.5 km in depth, where the black, red, and green lines denote the trace from the PWM image, the FWM image, and the FWM image after LPMO, respectively, (b and c) local similarity maps before and after using LPMO on the FWM image, respectively, (d) estimated negative-only LPMO weight related to the transmission effects, (e) FWM image after conventional L_2 -norm adaptive subtraction of the difference image from Figure 1c, and (f) conventional L_2 -norm adaptive subtraction matched difference image.

primaries and multiples; therefore, an adaptive component from LPMO to improve its results will be playing a crucial role in its acceptance and success.

Regarding the general applicability of the proposed framework, on the one hand, we are currently working on a version in which reverse time migration (RTM) is the main engine and multiples are explained on the fly as part of the traditional RTM-based imaging process. From this perspective, the proposed methodology can be applied to RTM-type methods. However, whether our proposed methodology is generally applicable to other traditional imaging methods depends on their own ability to handle internal multiples during imaging. For example, conventional RTM cannot include

internal multiples during the imaging process. Thus, we cannot directly apply our proposed framework on conventional RTM. However, if conventional RTM is combined with any conventional internal multiple removal technique, our proposed framework can definitely be applicable. Specifically, the internal multiples can be first attenuated in the data domain before RTM and then RTM can produce an image with internal multiples attenuated. In this way, one can obtain two RTM images with and without internal multiples. Accordingly, a difference image with the estimated internal multiples can be achieved, and the internal multiple crosstalk in the RTM image can be further matched and attenuated using the difference image based on LPMO. Note that the transmission effects

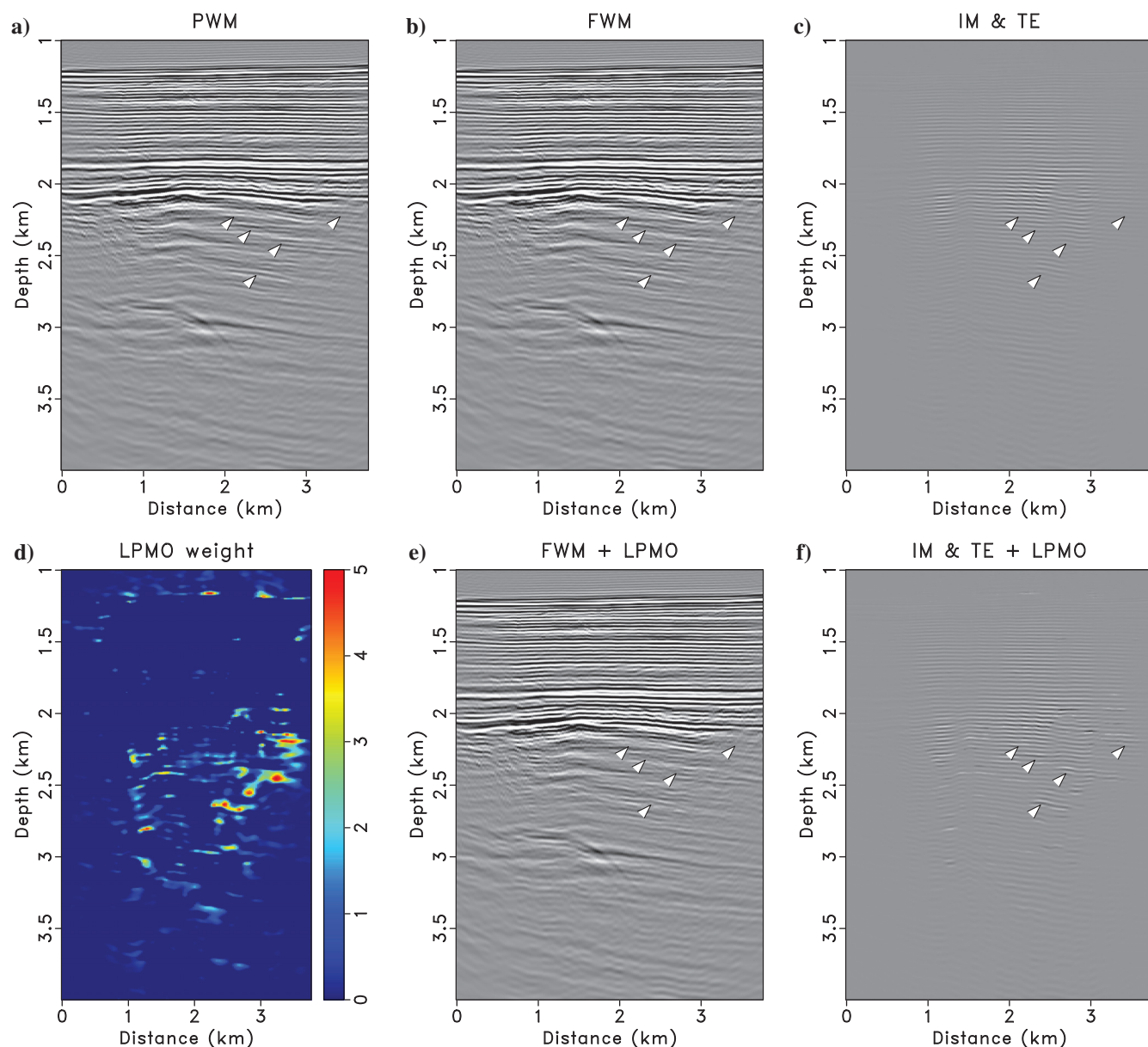


Figure 3. LPMO on the FWM image of the Vøring field data set with 3% velocity errors: (a) PWM image, (b) FWM image, (c) the difference image between PWM and FWM that includes the initially estimated internal multiples and transmission effects, (d) estimated positive-only LPMO weight related to the leaked internal multiple crosstalk in the FWM image, (e) final estimated FWM image after LPMO, and (f) the difference image that includes the final estimated internal multiples and transmission effects after LPMO.

will not be taken into consideration by conventional RTM. Still, LPMO will outperform the L_2 -norm adaptive subtraction in terms of internal multiple crosstalk attenuation due to its nonstationary property. Besides, our proposed framework is also useful for those model-based internal multiple removal methods as long as the estimated internal multiples are available.

Although all of the examples are shown for 2D data, this framework can be straightforwardly extended to the 3D case. The 3D FWM has already been demonstrated, and the details can be found in Davydenko and Verschuur (2017). As for LPMO, it is also straightforward to extend to the 3D case. In fact, the LPMO formulas in equations 4–6 do not have any limitations on the dimension. However, the computational cost might be an issue due to the smoothing process inside the shaping regularization-based inversion. Thus, we could still consider LPMO on 3D data in a 2D manner (i.e., data slice by slice) in terms of the efficiency. An extended image domain (e.g., by angle-dependent FWM [Davydenko and Verschuur, 2018]) might produce even better results than the original image domain. However, we still need to consider the issue of the increased computational cost of LPMO from one image to hundreds of image gathers. Besides, although we ignore elastic effects, we do include multiple scattering and transmission effects that other methods usually ignore. Note that the anelastic Q -effect is another factor on top of the regular transmission effect, and this can be included in our FWM method by including it in the propagator (Alasmri and Verschuur, 2019), without influencing our proposed framework.

CONCLUSION

We have shown that the positive LPMO weight is able to estimate the leaked internal multiple crosstalk from an FWM image, whereas the negative LPMO weight indicates the transmission effects. From the Vøring field data set application, it has been demonstrated that the leaked internal multiple crosstalk in the FWM image can be further attenuated to a minimum by the LPMO process. The proposed framework, that is, generating PWM and FWM outputs and then using LPMO on the FWM image, should be considered as a routine procedure for internal multiple imaging, where LPMO could also be regarded as a QC step on the FWM image.

ACKNOWLEDGMENTS

The authors would like to thank the editor-in-chief J. Shragge for his careful revision in the final phase, the associate editor N. Grobbe, the assistant editor J. Blanch, and three other anonymous reviewers for their helpful suggestions. D. Zhang, D. J. Verschuur, M. Davydenko, A. M. Alfaraj, and S. Qu thank the sponsors of the

Delphi Consortium for their support. Y. Chen is supported by the Starting Funds from Zhejiang University. The authors would like to thank Equinor for providing the field data set.

DATA AND MATERIALS AVAILABILITY

Data associated with this research are available and can be obtained by contacting the corresponding author.

REFERENCES

- Alasmri, H., and D. J. Verschuur, 2019, Towards Q-compensation in full wavefield migration and joint migration inversion: 81st Annual International Conference and Exhibition, EAGE, Extended Abstracts, Tu_R01_11, doi: [10.3997/2214-4609.201900787](https://doi.org/10.3997/2214-4609.201900787).
- Berkhout, A. J., 2014a, Review paper: An outlook on the future of seismic imaging — Part 1: Forward and reverse modelling: *Geophysical Prospecting*, **62**, 911–930, doi: [10.1111/1365-2478.12161](https://doi.org/10.1111/1365-2478.12161).
- Berkhout, A. J., 2014b, Review paper: An outlook on the future of seismic imaging — Part 2: Full-wavefield migration: *Geophysical Prospecting*, **62**, 931–949, doi: [10.1111/1365-2478.12154](https://doi.org/10.1111/1365-2478.12154).
- Chen, Y., and S. Fomel, 2015, Random noise attenuation using local signal-and-noise orthogonalization: *Geophysics*, **80**, no. 6, WD1–WD9, doi: [10.1190/geo2014-0227.1](https://doi.org/10.1190/geo2014-0227.1).
- Davydenko, M., and D. J. Verschuur, 2017, Full-wavefield migration: Using surface and internal multiples in imaging: *Geophysical Prospecting*, **65**, 7–21, doi: [10.1111/1365-2478.12360](https://doi.org/10.1111/1365-2478.12360).
- Davydenko, M., and D. J. Verschuur, 2018, Including and using internal multiples in closed-loop imaging — Field data examples: *Geophysics*, **83**, no. 4, R297–R305, doi: [10.1190/geo2017-0533.1](https://doi.org/10.1190/geo2017-0533.1).
- Fomel, S., 2007a, Local seismic attributes: *Geophysics*, **72**, no. 3, A29–A33, doi: [10.1190/1.2437573](https://doi.org/10.1190/1.2437573).
- Fomel, S., 2007b, Shaping regularization in geophysical-estimation problems: *Geophysics*, **72**, no. 2, R29–R36, doi: [10.1190/1.2433716](https://doi.org/10.1190/1.2433716).
- Jakubowicz, H., 1998, Wave equation prediction and removal of interbed multiples: 68th Annual International Meeting, SEG, Expanded Abstracts, 1527–1530, doi: [10.1190/1.1820204](https://doi.org/10.1190/1.1820204).
- Pica, A., and L. Delmas, 2008, Wave equation based internal multiple modeling in 3D: 78th Annual International Meeting, SEG, Expanded Abstracts, 2476–2480, doi: [10.1190/1.3063858](https://doi.org/10.1190/1.3063858).
- van der Neut, J., and K. Wapenaar, 2016, Adaptive overburden elimination with the multidimensional Marchenko equation: *Geophysics*, **81**, no. 5, T265–T284, doi: [10.1190/geo2016-0024.1](https://doi.org/10.1190/geo2016-0024.1).
- Verschuur, D. J., and A. J. Berkhout, 2005, Removal of internal multiples with the common-focus-point (CFP) approach: Part 2 — Application strategies and data examples: *Geophysics*, **70**, no. 3, V61–V72, doi: [10.1190/1.1925754](https://doi.org/10.1190/1.1925754).
- Wang, B., J. Cai, M. Guo, C. Mason, S. Gajawada, and D. Epili, 2011, Postmigration multiple prediction and removal in the depth domain: *Geophysics*, **76**, no. 5, WB217–WB223, doi: [10.1190/geo2011-0010.1](https://doi.org/10.1190/geo2011-0010.1).
- Weglein, A. B., F. A. Gasparotto, P. M. Carvalho, and R. H. Stolt, 1997, An inverse-scattering series method for attenuating multiples in seismic reflection data: *Geophysics*, **62**, 1975–1989, doi: [10.1190/1.1444298](https://doi.org/10.1190/1.1444298).
- Zhang, D., D. J. Verschuur, S. Qu, and Y. Chen, 2020, Surface-related multiple leakage extraction using local primary-and-multiple orthogonalization: *Geophysics*, **85**, no. 1, V81–V97, doi: [10.1190/geo2019-0465.1](https://doi.org/10.1190/geo2019-0465.1).
- Zhang, L., and E. Slob, 2019, Free-surface and internal multiple elimination in one step without adaptive subtraction: *Geophysics*, **84**, no. 1, A7–A11, doi: [10.1190/geo2018-0548.1](https://doi.org/10.1190/geo2018-0548.1).

Biographies and photographs of the authors are not available.